

Figure 1. Probabilistic bit measurements. Top: reference distributions of the ensemble in zero field $B = 0$, initial temperature T and the beginning of timekeeping $t = 0$. Bottom: deviated distributions in the presence of magnetic field $B \neq 0$, temperature change δT and time elapse $t > 0$.

extract information about β or U . Since the p-bits keep fluctuating, the measured number n also fluctuates. However, the uncertainty in n due to this fluctuation is proportional to the square root of the total number: $\delta n \propto \sqrt{N}$. Therefore, for sufficiently large N , the mean value of the population imbalance can always overshadow the uncertainty: $n > \delta n$, thus enabling the p-bit ensemble for the purpose of measurement.

Based on this simple principle, we explore the possibility and practicality of probabilistic measurement (p-measurement), and propose strategies that leverage p-bits for various purposes. Compared to some previous works that use noisy or chaotic systems for magnetic field sensing [16, 17], temperature monitoring [18] and timekeeping [19–21], the outlined measurement methodologies put emphasis on bistable systems (bits) while preserving the exploitation of randomness. The principles are delineated in Fig. 1, where the field sensing and temperature variation monitoring make use of equilibrium states of the p-bit ensemble and the timekeeping relies on transient states.

Field sensing - For magnetic field sensing, an ensemble of p-bits initially assume a state of equilibrium characterized by an even distribution of 0s and 1s (with $U = 0$), albeit within a certain statistical margin of error. Upon the introduction of an external magnetic field denoted as B , an energy bias $U = 2MB$ emerges between the state-0 and the state-1, prompting an asymmetry in the quantities N_0 and N_1 as expressed in Eq. (1). By measuring the imbalance $n = N_0 - N_1$, it becomes feasible to deduce the intensity of the magnetic field.

Temperature monitoring - In a manner analogous to field sensing, it is possible to determine the temperature based on the energy bias $U \neq 0$ and the measured quantities N_0 and N_1 . However, this approach necessitates prior knowledge of the energy bias U , which is a parameter that may not be readily available and could vary from one p-bit to another. Consequently, it is not practical to directly ascertain the absolute temperature using p-bits. However, it is feasible to

accurately gauge the variations in temperature without precise knowledge of potentially non-constant device parameters like U . For a collection of p-bits with an energy bias of U , the population imbalance n is contingent upon temperature. As the temperature rises, the population in state-1 also increases. By measuring the alteration in population imbalance $\delta n = n_{T'} - n_T$, it is possible to infer the temperature change $\delta T = T' - T$.

Timekeeping - Timekeeping is yet another task that can be achieved probabilistically. Most timekeeping devices rely on some kind of oscillating phenomena with fixed periods. From the rhythmic swings of a pendulum to the consistent vibrations of quartz crystals and the intricate quantum transitions between energy levels, these mechanisms serve as the foundation for tracking time by counting cycles. However, a unique form of timekeeping makes use of the radioactive decay of certain atoms, notably Carbon-14 (^{14}C). While this method may not boast the same level of precision as its counterparts, it stands out for its simplicity and resilience against various external disturbances. An ensemble of p-bits can emulate the behavior of radioactive atoms. The timekeeping is initialized by resetting all p-bits into one single state (say the 0 state). Afterwards, the ensemble undergoes thermal fluctuation and would eventually approach the thermal equilibrium on a time scale comparable to the thermalization time. Therefore, it is possible to estimate the elapsed time by counting the number of p-bits in state-1. Here the thermalization of p-bit is equivalent to the radioactive decay of ^{14}C . The thermalization time for a p-bit, equivalent to the half-life of ^{14}C , is dictated by the energy barrier $\tau \propto \exp(\beta\Delta)$ and can vary significantly, ranging from sub-microseconds to years.

Realization with MTJ p-bits - We now consider a possible realization of the probabilistic measurement utilizing the p-bits based on the magnetic tunnel junction (MTJ) [22–25]. We assume a typical MTJ p-bit with the following parameters: the free layer magnetization has total magnetization of $M = M_s V$ with volume V and saturation magnetization M_s , and the barrier separating the two equilibrium states is $\Delta = KM$ with anisotropy K . We shall assume that $\Delta/k_B T \lesssim 10$ for enabling fast thermal fluctuation. In the absence of external magnetic fields, the MTJ p-bit fluctuates between parallel (0) and anti-parallel (1) state with equal probability.

Field Sensing - In order to measure weak magnetic fields, the p-bit must respond to the external field. As shown in Fig. 1(a), the magnetic field B along the anisotropy direction gives rise to an energy bias $U_B = MB$ between the parallel and anti-parallel state, which leads to an imbalance of the MTJ p-bits

$$n_B = N \tanh(\beta MB) \simeq N\beta MB \equiv \chi_B B, \quad (2)$$

where $\chi_B = N\beta M$ is the susceptibility of the imbalance in response to a small external field B . The statistical fluctuation of the p-bits is roughly

$$\delta n = 2\sqrt{N_0 N_1 / N} = \sqrt{N} \operatorname{sech}(\beta MB) \simeq \sqrt{N}, \quad (3)$$

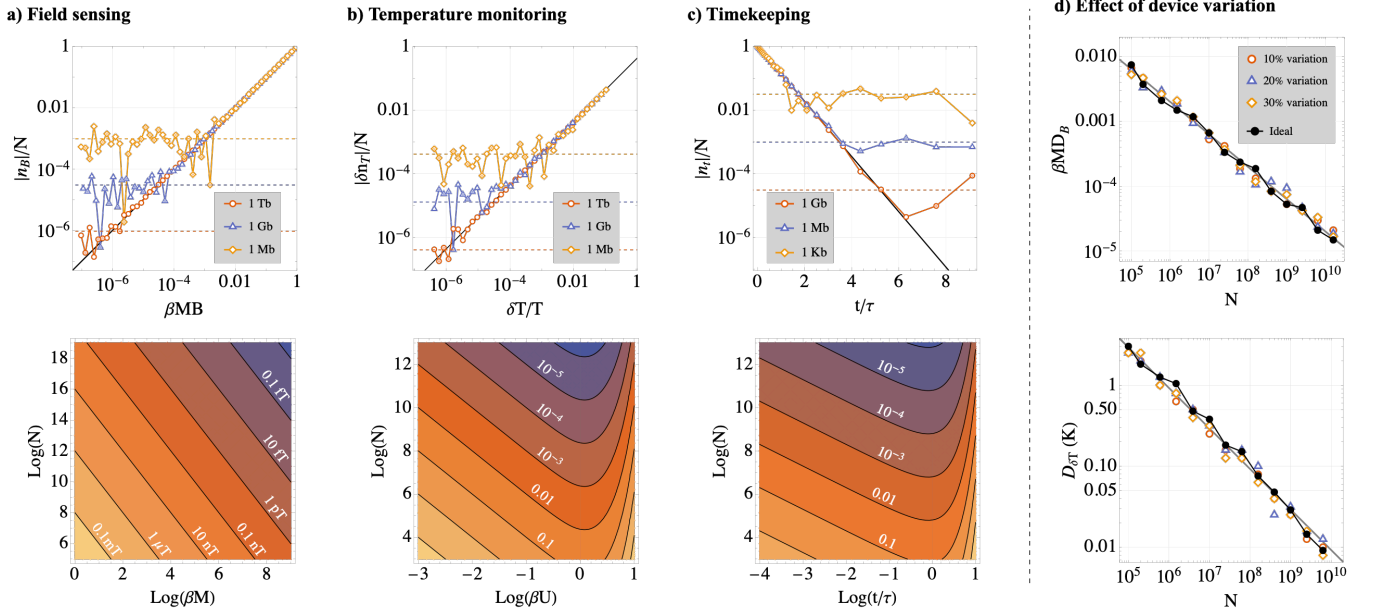


Figure 2. a) Upper: Simulation result of imbalance $|n_B|$ as a function of dimensionless field βMB for $N = 10^6$ (1 Mb), 10^9 (1 Gb) and 10^{12} (1 Tb); Lower: Theoretical prediction of field detectivity D_B in Eq. (4) as a function of N and total magnetization βM . The negative n_B values are marked with double open symbols. b) Upper: Simulated change of imbalance $|\delta n_T|$ as a function of relative temperature change $\delta T/T$ for $\beta U = 1$ and room temperature ($T = 300$ K); Lower: Predicted temperature detectivity $D_{\delta T}/T$ in Eq. (8) as a function of N and barrier height βU at room temperature. The optimal choice is at $\beta U = 1.2$. c) Upper: Simulated imbalance $|n_t|$ as a function of dimensionless time t/τ ; Lower: Predicted temporal detectivity D_t/t in Eq. (12) as a function of N and time t . d) The effect of device-to-device variation of p-bits on the overall performance for field sensing (upper) and room temperature monitoring (lower).

which equals to \sqrt{N} when the external field is weak. Therefore, when the field induced imbalance is greater than the fluctuations $|n_B| > |\delta n|$, the external field can be distinguished by the imbalance n_B . The weakest detectable field, or the field detectivity D_B , is given by

$$D_B = \frac{\delta n}{\chi_B} = \frac{1}{\sqrt{N}} \frac{k_B T}{M_s V}. \quad (4)$$

The upper panel of Fig. 2(a) shows the readout of n_B as function of external magnetic field for $N = 1$ Mb, 1 Gb, 1 Tb, respectively. The lower panel of Fig. 2(a) shows the field detectivity Eq. (4) as a function of βM and N . Eq. (4) shows that increasing the total magnetization $M_s V$ is more effective in enhancing the field sensitivity than increasing p-bit number N . However, the larger magnetization would suppress the magnetization fluctuation. As shown by Chen *et. al.* [26], this contradiction can be resolved by applying a transverse magnetic field to reduce the potential barrier between the 0 and 1 state, thus enhancing the fluctuation rate significantly. Based on a MTJ with $M_s = 9.6 \times 10^5$ A/m and $V = 10^4$ nm³ [27, 28], $k_B T/M \sim 0.3$ mT in room temperature, thus a field sensitivity of 1 nT can be achieved with $N \sim 100$ Gb outputs from p-bits at room temperature.

Temperature Monitoring - We now consider biased p-bits whose parallel and anti-parallel configurations have energy difference of $2U$. The bias can be implemented by some intrinsic pinning within the MTJ or by applying a fixed external

field. Because of the energy difference, the imbalance at thermal equilibrium is non-zero (at temperature T):

$$n_T = N_1(T) - N_0(T) = -N \tanh(\beta U). \quad (5)$$

A temperature change δT will cause a change in n_T by

$$\delta n_T = \frac{\partial n_T}{\partial T} \delta T = N \beta U \operatorname{sech}^2(\beta U) \frac{\delta T}{T} = \chi_\tau \frac{\delta T}{T}. \quad (6)$$

Here $\chi_\tau \simeq N \beta U$ is the susceptibility of the imbalance in response to the temperature variation $\delta T/T$. In the mean time, the statistical fluctuation in n_T is roughly

$$\delta n \simeq 2\sqrt{N p_0 p_1} = 2\sqrt{N_0 N_1 / N} = \sqrt{N} \operatorname{sech}(\beta U). \quad (7)$$

When the temperature-change induced imbalance-change exceeds the statistical fluctuation $|\delta n_T| > |\delta n|$, the temperature change can be inferred from δn_T . This also defines the minimum temperature change detectable, or the temperature detectivity $D_{\delta T}$

$$\frac{D_{\delta T}}{T} = \frac{\delta n}{\chi_\tau} = \frac{\cosh(\beta U)}{\beta U \sqrt{N}} \gtrsim \frac{1.5}{\sqrt{N}}. \quad (8)$$

The lower bound in Eq. (8) happens at $\beta U \simeq 1.2$. The upper panel of Fig. 2(b) shows the readout of δn_T as a function of temperature variation δT . The lower panel of Fig. 2(b) shows the temperature detectivity Eq. (8) as a function of βU and N ,

according to which a temperature variation of ~ 1 mK at room temperature can be detected with $N = 200$ Gb of p-bits and $\beta U = 1$.

Timekeeping - In order to use p-bits for timekeeping, an ensemble of unbiased p-bits is first initialized by resetting them to state-0 at $t = 0$, such that the initial imbalance $n = N_0 - N_1 = N$ maximizes. Afterwards, the thermalization process will drive the system towards a balanced distribution with $n \sim 0$. During the thermalization process, the imbalance decreases exponentially as function of time:

$$n_t = N_0(t) - N_1(t) = N e^{-t/\tau}, \quad (9)$$

where $\tau \propto e^{\beta \Delta}$ is the thermalization time, or the half-life of p-bits. By measuring the imbalance n_t at a later time, the time t elapsed since the initialization can be inferred as:

$$t = -\tau \ln(n_t/N). \quad (10)$$

The statistical fluctuation in n_t is given by

$$\delta n_t = 2\sqrt{N_0 N_1 / N} \simeq \sqrt{N(1 - e^{-2t/\tau})}, \quad (11)$$

and the relative uncertainty δt (detectivity D_t) is

$$\frac{D_t}{t} = \frac{\delta t}{t} = \left| \frac{\partial t}{\partial n_t} \right| \frac{\delta n_t}{t} = \frac{\tau}{t} \sqrt{\frac{e^{2t/\tau} - 1}{N}}, \quad (12)$$

which reaches its minimum when the elapsed time is comparable to half-life of the p-bits. The upper panel of Fig. 2(c) shows the readout of n_t as a function of time t , which shows that merely 1 Kb p-bits can already make a timekeeping on the time scale of one half-life. The lower panel of Fig. 2(c) shows uncertainty in time Eq. (12) as a function of elapsed time t and bit number N .

Efficient read-out - Traditionally, the determination of imbalance in a system comprising N p-bits requires reading all p-bits, which is notably time-consuming. Fortunately, since the specific states of the p-bits (whether 0 or 1) are irrelevant to the imbalance, it is feasible to ascertain this information through minimal measurements. By arranging the p-bits in a $P \times Q = N$ series-parallel circuit configuration [23], the imbalance is intricately linked to the overall resistance of the circuit. Let r and R be the resistance of the MTJ p-bit in the parallel (0) and anti-parallel (1) states. Suppose the i -th branch has N_0^i p-bits in r and N_1^i in R with $P = N_0^i + N_1^i$ and $n_i \equiv N_1^i - N_0^i \ll P$, and the total resistance of the series-parallel circuit is

$$R_{sp} = \left(\sum_{i=1}^Q \frac{1}{N_0^i r + N_1^i R} \right)^{-1} \simeq \frac{R+r}{2Q/P} \left(1 + \frac{R-r}{R+r} \frac{n}{N} \right), \quad (13)$$

which establishes a one-to-one association between R_{sp} and the imbalance $n = \sum_i n_i = N_1 - N_0 \ll N$. The exact partition of the p-bits for P and Q can be tuned according to the range and precision of resistance measurement. This approach

not only simplifies the process but also significantly reduces the time and resources needed for determining the imbalance.

Influence of imperfections of p-bits - To achieve higher measurement accuracy, traditional methods typically rely on the enhancement of instrument or device quality. However, the probabilistic measurements discussed in this Letter deviate from this norm. Here, accuracy is improved by increasing the quantity of p-bits rather than by refining the quality of each individual p-bit. This methodology not only proves to be more cost-effective but also enhances flexibility and scalability across various applications. As demonstrated in Fig. 2(d), discrepancies among p-bits, simulated through parameter variations like M, β, B, U by up to $\pm 30\%$, do not adversely affect the measurement sensitivity. This robustness stems from the error-cancelling effect achieved when employing a large ensemble of p-bits.

Discussion - The concept of probabilistic field sensing hinges on the ability to achieve remarkably high sensitivity levels, contingent upon the acquisition of substantial data volumes, as illustrated in Fig. 2(a). Specifically, with an N value approximating 10^{20} , or equivalently 10^8 Tb, femto-Tesla sensitivity becomes attainable. This can be realized through repeated measurement of a series-parallel circuit of a p-bit array, where N represents the cumulative total of the p-bits in the circuit multiplied by the number of measurement iterations. Conversely, temperature monitoring demands a significantly lower number of p-bits – mere gigabits suffice to achieve a sensitivity of 10 mK at room temperature. While probabilistic timekeeping may not rival the precision of atomic clocks or conventional timepieces in terms of accuracy, its simplicity in design and robustness against non-uniformity and disturbances make it a viable option. Requiring around 1 Kb independent p-bits, probabilistic timekeeping is particularly conducive to biomorphic implementations [29]. The discussion thus far has centered on probabilistic measurements utilizing independent p-bits. Given the nature of probabilistic computing, which involves interconnecting p-bits into a network, it prompts an inquiry into how such interconnected p-bits might enhance measurement sensitivity in probabilistic systems.

In conclusion, we proposed an innovative probabilistic measurement framework utilizing an ensemble of p-bits. This approach was demonstrated to be effective in applications such as field sensing, temperature variation monitoring and timekeeping. Notably, by augmenting the total number of p-bits, we can attain unprecedented sensitivity in these domains. Furthermore, the requisite quality and uniformity of the p-bits are not critical factors for achieving high sensitivity, which significantly enhances the scalability of our proposed scheme.

Acknowledgements - This work was supported by the National Key Research and Development Program of China (Grant no. 2022YFA1403300) and Shanghai Municipal Science and Technology Major Project (Grant No.2019SHZDZX01).

* Corresponding author: xiaojiang@fudan.edu.cn

- [1] M. A. Nielsen and I. L. Chuang, *Quantum computation and quantum information* (Cambridge university press, Cambridge, 2010), 10th ed.
- [2] C. Degen, F. Reinhard, and P. Cappellaro, *Rev. Mod. Phys.* **89**, 035002 (2017).
- [3] V. Giovannetti, S. Lloyd, and L. Maccone, *Science* **306**, 1330 (2004).
- [4] V. Giovannetti, S. Lloyd, and L. Maccone, *Phys. Rev. Lett.* **96**, 010401 (2006).
- [5] D. Feng, *IOP Conf. Ser.: Earth Environ. Sci.* **237**, 032027 (2019).
- [6] F. Riehle, *Nature Photonics* **11**, 25 (2017).
- [7] S. Beattie, B. Jian, J. Alcock, and M. Gertszvol, *Canadian Journal of Physics* **101**, 53 (2023).
- [8] *Phys. Rev. Lett.* **116**, 061102 (2016).
- [9] K. Camsari and S. Datta, *IEEE Spectr.* **58**, 30 (2021).
- [10] J. Kaiser and S. Datta, *Appl. Phys. Lett.* **119**, 150503 (2021).
- [11] W. A. Borders, A. Z. Pervaiz, S. Fukami, K. Y. Camsari, H. Ohno, and S. Datta, *Nature* **573**, 390 (2019).
- [12] K. Y. Camsari, B. M. Sutton, and S. Datta, *Applied Physics Reviews* **6**, 011305 (2019).
- [13] S. Chowdhury, A. Grimaldi, N. A. Aadit, S. Niazi, M. Mohseni, S. Kanai, H. Ohno, S. Fukami, L. Theogarajan, G. Finocchio, et al., *IEEE Journal on Exploratory Solid-State Computational Devices and Circuits* pp. 1–1 (2023).
- [14] J. Kim, J.-K. Han, H.-Y. Maeng, J. Han, J. W. Jeon, Y. H. Jang, K. S. Woo, Y.-K. Choi, and C. S. Hwang, *Advanced Functional Materials* (2024).
- [15] J. Chou, S. Bramhavar, S. Ghosh, and W. Herzog, *Scientific Reports* **9** (2019).
- [16] A. Grigorenko, P. Nikitin, and G. Roschepkin, *Sensors and Actuators A - Physical* **59**, 277 (1997).
- [17] I. G. Silva, W. Korneta, S. G. Stavrinides, R. Picos, and L. O. Chua, *Communications in Nonlinear Science and Numerical Simulation* **94** (2021).
- [18] S. P. Benz, K. J. Coakley, N. E. Flowers-Jacobs, H. Rogalla, W. L. Tew, J. Qu, D. R. White, C. Gaiser, A. Pollarolo, and C. Urano, *Metrologia* **61** (2024).
- [19] M. Aitken, *Reports on Progress in Physics* **62**, 1333 (1999).
- [20] P. Di Lazzaro, A. C. Atkinson, P. Iacomussi, M. Riani, M. Ricci, and P. Wadhams, *Entropy* **22** (2020).
- [21] D. D. McCarthy and P. K. Seidelmann, *Time: From Earth Rotation to Atomic Physics* (Cambridge University Press, 2018), 2nd ed.
- [22] S. Yan, Z. Zhou, Y. Yang, Q. Leng, and W. Zhao, *Tsinghua Science and Technology* **27**, 443 (2022).
- [23] R. Guerrero, M. Pannetier-Lecoecur, C. Fermon, S. Cardoso, R. Ferreira, and P. P. Freitas, *Journal of Applied Physics* **105** (2009).
- [24] M. Oogane, K. Fujiwara, A. Kanno, T. Nakano, H. Wagatsuma, T. Arimoto, S. Mizukami, S. Kumagai, H. Matsuzaki, N. Nakasato, et al., *Applied Physics Express* **14** (2021).
- [25] A. Sengupta, C. M. Liyanagedera, B. Jung, and K. Roy, *Scientific Reports* **7** (2017).
- [26] X. Chen, J. Zhang, and J. Xiao, *Phys. Rev. Applied* **18**, L021002 (2022).
- [27] H. Zhao, A. Lyle, Y. Zhang, P. K. Amiri, G. Rowlands, Z. Zeng, J. Katine, H. Jiang, K. Galatsis, K. L. Wang, et al., *Journal of Applied Physics* **109** (2011).
- [28] D. Vodenicarevic, N. Locatelli, A. Mizrahi, J. S. Friedman, A. F. Vincent, M. Romera, A. Fukushima, K. Yakushiji, H. Kubota, S. Yuasa, et al., *Physical Review Applied* **8** (2017).
- [29] D. Buonomano, *Your brain is a time machine: the neuroscience and physics of time* (W. W. Norton & Company, New York, 2017), first edition ed.